Investigation of steady-state tyre force and moment generation under combined longitudinal and lateral slip conditions

Investigation of steady-state tyre force and moment generation under combined longitudinal and lateral slip conditions

GEORGE MAVROS, HOMER RAHNEJAT AND PAUL KING[1]

SUMMARY

The paper provides an insight into the contact mechanical behaviour of pneumatic tyres in a wide range of steady-state operating conditions. Tyre forces and self-aligning moment generation during steady-state manoeuvres are studied in some depth. For this purpose, two different versions of a dynamic model of a tyre are developed. The simplest version consists of a one-dimensional series of bristles distributed on the tyre periphery. The bristles incorporate anisotropic stiffness and damping in the lateral and longitudinal directions, while the distributed tread mass is also taken into account. The vertical pressure distribution along the contact patch is assumed to be parabolic and the length of the contact area is assumed to be known apriori. The friction forces developed on the contact patch follow a stick-slip friction law.

The second version of the tyre model improves the potential of the simple model by introducing radial and tangential stiffness and damping, as well as a Kelvin element for rubber behaviour in the simulation of the impact on the leading edge of the contact area. The Kelvin model closely conforms to the semi-infinite incompressible nature of rubber. The tyre models show effective reproduction of measured longitudinal and lateral forces, as well as the self-aligning moment, under pure side-slip, pure longitudinal slip and combined slip situations. The generated curves show qualitative concordance with the results obtained experimentally, or by semi-empirical models such as the Pacejka's Magic Formula. In addition, the tyre models seem to be capable of reproducing the generated contact pressure profiles and the shape of the observed variations in tyre forces between side-slipping, braking and traction diagrams. An investigation of these three situations reveals the different mechanisms that result in the different shapes of the diagrams.

Finally, a study is carried out for tyre behaviour at very high speeds, which indicates deviations from the results of traditional investigations.

1 INTRODUCTION

The primary aim in any tyre analysis is the prediction of tyre forces and moments applied on the wheel-hub, under various driving conditions. Due to the highly non linear and interdependent nature of these forces, it is often necessary to look into a number of different aspects of tyre behaviour.

Pacejka and Sharp [1] provide with a comprehensive review of modelling aspects depicting all the current trends in steady state tyre modelling. Increasingly complex points of view are presented, including anisotropic tyre behaviour, various shapes of contact pressure distribution, tyre belt deformation and camber angle effects. It is

[1] Wolfson School of Mechanical and Manufacturing Eng. Loughborough University LE11 3TU, UK

evident that the use of brush-type models has enhanced our understanding of tyre behaviour and has also contributed in the area of tyre simulation. Sakai [2-5] provides with a detailed analysis on tyre force generation, covering almost all aspects of it. The author's investigations start from basic definitions and the presentation of simple tyre models. The frictional behaviour of rubber, the shape of the contact pressure distribution and some experimental and simulation techniques are also discussed. Bernard et al [6] use a brush model accompanied by a simple friction law and a normal pressure distribution known beforehand in order to develop a tyre model appropriate for computer simulation. Sharp et al [7] use a multi-spoke model that is able to generate tyre shear forces as well as the normal pressure distribution, while Levin [8] uses an anisotropic brush model with distributed mass that emphasises on the shape of the pressure distribution and the generation of tyre forces in high speeds.

The models presented in this paper attempt to enhance understanding of tyre behaviour under various driving conditions. A critical view is maintained and the effects of different assumptions are discussed in detail. Some limitations of the brush models are presented and the effect of high rolling velocities is also investigated.

2 DESCRIPTION OF THE SIMPLE VERSION OF THE TYRE MODEL

2.1 Modelling of the tyre

The behaviour of tyre can be ascertained by discretisation of the continuum, as is the case for all contact mechanical treatments. The generation of shear forces is based on the brush concept. The tyre tread is modelled as a one-dimensional series of bristles distributed on the tyre periphery. The bristles incorporate anisotropic stiffness and damping in the lateral and longitudinal directions and the distributed tread mass on the tyre periphery is also taken into account by attaching an infinitesimal mass to the end of each bristle. Initially, for the sake of simplicity, the length of the contact patch is assumed constant and the vertical pressure distribution is regarded as parabolic.

All tyre properties are expressed per unit length of the tread. The mass distribution along the tyre tread is $C = dm / dx$, the stiffness coefficients per unit tread length are $K_x = dF/dxdx$, $K_y = dF/dydx$ for the longitudinal and lateral deformations of the bristles respectively, and the coefficients of damping are $D_x = dF/du_x dx$, $D_y = dF/du_y dx$, where u_x, u_y denote the rate of change of the longitudinal and lateral deformations of the bristles respectively.

Figure 1 shows a side view of the tyre model including the normal pressure distribution, and a top view of the model, depicting an arbitrary position of the infinitesimal mass dm, which corresponds to a length dx of the tyre tread. A bristle connecting the mass to the wheel periphery, is deformed laterally as well as

longitudinally and, the mass may or may not be sliding on the ground, depending on the forces applied by the bristle (viscoelastic element), the vertical force at the specific position and the local coefficient of friction.

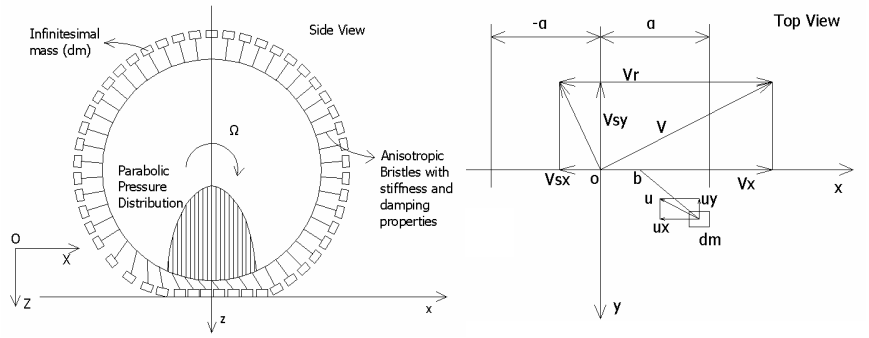

Fig. 1. Side and Top view of the tyre model, depicting an arbitrary position of infinitesimal mass.

The equation of the parabola, yielding the vertical force distribution per tyre tread length can be easily derived, given the length of the contact patch $l = 2 \cdot \alpha$ and taking into account the fact that the integral of the force along the contact patch balances the normal load applied on the wheel hub by the suspension:

$$F_{vertical} = \frac{3 \cdot F_z}{4 \cdot \alpha} \cdot \left(1 - \frac{x}{a}\right)^2 \tag{1}$$

where F_z denotes the total vertical force applied on the wheel hub.

Two different sets of axes are used in order to describe the motion of the tyre and its components. The global frame of reference (O, X, Y, Z) is attached to the ground, while a second frame of reference (o, x, y, z) has its origin on a point in the contact patch, where the vertical line from the centre of the wheel plane meets the ground. Both frames are shown in Figure 1.

The longitudinal component of the velocity of the bristle base relative to the ground (i.e. in the global frame of reference) is V_{sx}, the lateral component being V_{sy}. When the vertical force results in the generation of a high enough frictional force the infinitesimal mass *dm* sticks to the ground. In any other case, the mass moves with

respect to the ground with a sliding velocity u, consisting of u_x and u_y in the longitudinal and lateral directions respectively.

For the purpose of the analysis, the motion of the infinitesimal mass is traced throughout the contact patch and beyond the end of it. The analysis, therefore, considers the physics of motion of a typical infinitesimal mass through the contact to be representative of all such discrete elements. Thus, the proposed model represents steady state contact conditions.

2.2 Modelling of friction

Friction f between the infinitesimal mass and the road is assumed to follow a stick-slip friction law. Karnopp [9] provides with a way of modelling the stick-slip behaviour for use in computer simulations. This approach is valid for hard, almost elastic materials such as steel. Visco-elastic materials with low stiffness and considerable internal damping (such as rubber) show a more complicated frictional behaviour that strongly depends on the vertical load, apparent contact area, sliding velocity and temperature [2]. Nevertheless, experimental work [10] indicates that stick-slip behaviour is not only evident in rubber contacts, but in some cases the friction laws appear to be very similar to the laws describing hard materials. Thus, as a starting point for the present analysis, a typical stick-slip law is chosen with a transition between the static and a constant kinetic friction.

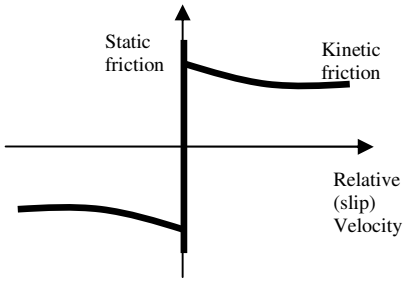

Fig. 2. Stick-Slip Friction Law.

2.3 Equations of motion for the infinitesimal mass

The motion of an infinitesimally small length dx of the tyre tread is considered. According to the definitions given previously for the mass, stiffness and damping distributions, the equations of motion of the infinitesimal mass dm which corresponds to length dx, are written as follows (in accordance with Figure 1):

$$\dot{u}_x \cdot C \cdot dx = (x_s - x) \cdot K_x \cdot dx + (V_{sx} - u_x) \cdot D_x \cdot dx - f_x \quad (2)$$

$$\dot{u}_y \cdot C \cdot dx = (y_s - y) \cdot K_y \cdot dx + (V_{sy} - u_y) \cdot D_y \cdot dx - f_y \quad (3)$$

Error! Objects cannot be created from editing field codes. (4)

$$\dot{y}_s = V_{sy} \quad (5)$$

where f_x, f_y denote the friction forces in the longitudinal and lateral directions respectively. Forces f_x and f_y depend on the normal force at the specified point of the contact patch, the friction coefficient and the direction of motion of the infinitesimal mass.

3 EXPANSION OF THE SIMPLE TYRE MODEL

A mechanism has to be incorporated in order to simulate the build-up of vertical pressure distribution on the tyre contact patch. For this purpose, a couple of modifications are made to the aforementioned simple model. First, radial and tangential stiffness and damping characteristics are introduced. Secondly, a Kelvin element is used to connect the infinitesimal mass to the ground. The Kelvin element is used mainly for the simulation of the impact of a viscoelastic solid, while the combined effect of tangential and radial compliance replaces the longitudinal stiffness and damping of the bristles. The modified tyre model is shown in Figure 3.

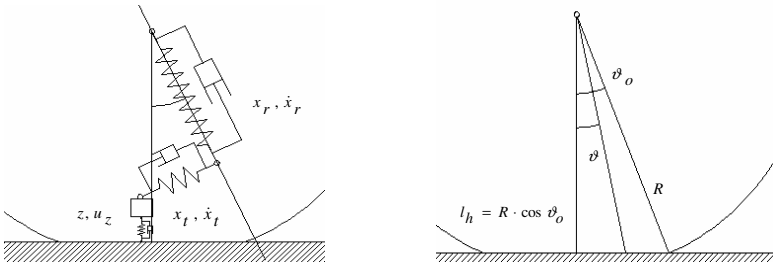

Fig. 3. The modified tyre model and some important dimensions

The derivation of the equations of motion for the infinitesimal mass is achieved by depicting a random position of the mass, after it has entered the contact patch. Referring to Figure 4, equations (2)-(5) can be re-written as follows:

$$\dot{u}_x \cdot C \cdot dx = K_r \cdot x_r \cdot \sin\vartheta \cdot dx - K_t \cdot x_t \cdot \cos\vartheta \cdot dx + D_r \cdot \dot{x}_r \cdot \sin\vartheta \cdot dx - D_t \cdot \dot{x}_t \cdot \cos\vartheta \cdot dx - f_x \tag{6}$$

$$\dot{u}_y \cdot C \cdot dx = (y_s - y) \cdot K_y \cdot dx + (V_{sy} - u_y) \cdot D_y \cdot dx - f_y \tag{7}$$

$$\dot{u}_z \cdot C \cdot dx = C \cdot g \cdot dx + K_r \cdot x_r \cdot \cos\vartheta \cdot dx + K_t \cdot x_t \cdot \sin\vartheta \cdot dx + D_r \cdot \dot{x}_r \cdot \cos\vartheta \cdot dx + D_t \cdot \dot{x}_t \cdot \sin\vartheta \cdot dx - K_z \cdot x_z \cdot dx - D_z \cdot u_z \cdot dx \tag{8}$$

$$\dot{x} = u_x \tag{9}$$

$$\dot{y} = u_y \tag{10}$$

$$\dot{z} = u_z \tag{11}$$

$$\dot{y}_s = V_{sy} \tag{12}$$

If the state variables of the dynamic system are chosen as $x, y, z, u_x, u_y, u_z, y_s, x_r, x_t$, it becomes obvious that the set of differential equations is insufficient to arrive at an analytic solution. Furthermore, the absence of variable x_s disables the definition of longitudinal slip.

The problem is solved by introducing a set of kinematic constraints. Referring to Figure 3, the radius of the tyre just before entering the contact patch of the vertically loaded rolling tyre is R. This radius is assumed to remain constant in the area outside the contact patch and equal to the radius of the unloaded tyre. The angle between R and the vertical line, connecting the tyre centre to the ground is ϑ_o. Given R, the height of the tyre centre above the ground is $l_h = R \cdot \cos\vartheta_o$. This height is assumed to be equal to the radius of the vertically loaded tyre under pure rolling conditions, R_d.

At an arbitrary position of the mass inside the contact patch, the total deflection ΔR is given by the following scalar constraint function:

$$\Delta R = R - R \cdot \frac{\cos\vartheta_o}{\cos\vartheta} \tag{13}$$

The vertical projection of the total deflection ΔR is:

$$\Delta R_{vertical} = \Delta R \cdot \cos\vartheta = R \cdot (\cos\vartheta - \cos\vartheta_o) \tag{14}$$

At any instance of time, $\Delta R_{vertical}$ is equal to the vertical deflection of the Kelvin element (i.e. the "local" deflection) added to the vertical components of the deflections of the radial and tangential elements (i.e. the "global" deformation of the continuum), as described in the following equation:

$$x_r \cdot \cos\vartheta + x_t \cdot \sin\vartheta + x_z = R \cdot (\cos\vartheta - \cos\vartheta_o) \tag{15}$$

Analogously, the horizontal components of the deflections of the radial and tangential elements are equal to $x_s - x$, which represent the distances between the base and the tip of the bristles, as defined previously for the simple tyre model. Consequently, the following constraint function also holds true:

$$x_r \cdot \sin\vartheta - x_t \cdot \cos\vartheta = x_s - x \tag{16}$$

Equations (15), (16), provide a way of expressing x_r, x_t with respect to x, x_s and ϑ, while their derivatives provide two more relations, which include velocities $\dot{x}_r, \dot{x}_t, \dot{\vartheta} = \omega$, as follows:

$$\dot{x}_r \cdot \sin\vartheta + x_r \cdot \omega \cdot \cos\vartheta - \dot{x}_t \cdot \cos\vartheta + x_t \cdot \omega \cdot \sin\vartheta = V_{sx} - u_x \tag{17}$$

$$\dot{x}_r \cdot \cos\vartheta - x_r \cdot \omega \cdot \sin\vartheta + \dot{x}_t \cdot \sin\vartheta + x_t \cdot \omega \cdot \cos\vartheta + u_z = -R \cdot \omega \cdot \sin\vartheta \tag{18}$$

Equations (15)-(18) result in the omission of variables $x_r, x_t, \dot{x}_r, \dot{x}_t$ and enable the formulation of the system of differential equations in a way that x_s is retained as a state variable, thus providing a means for the definition of longitudinal slip.

The rate of change of angle ϑ can be obtained by solving the equation of motion of the wheel for the rotational degree of freedom, while height l_h, or alternatively angle ϑ_o (for a given radius R) can be obtained by solving the equation of motion of the wheel for the vertical degree of freedom.

4 RESULTS AND DISCUSSION

A number of simulations were carried out using the 4th order fixed step Runge Kutta method to solve the non-linear system of differential equations. The various tyre parameters were chosen according to [2-5], [8] and [10].

Figure 4 shows a typical response of the tyre model in pure cornering conditions, while Figure 5 presents a typical braking force diagram and a case of combined braking and cornering. The force diagrams appear to be smooth and show qualitative

concordance with experimental and empirical curves. A good quantitative agreement with experiments was achieved by modifying tyre parameters; nevertheless a consistent parameter identification technique is yet to be developed.

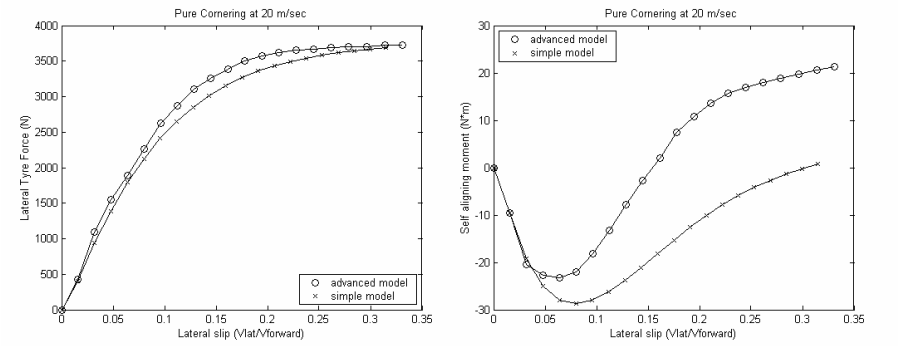

Fig. 4. Cornering force and self aligning moment

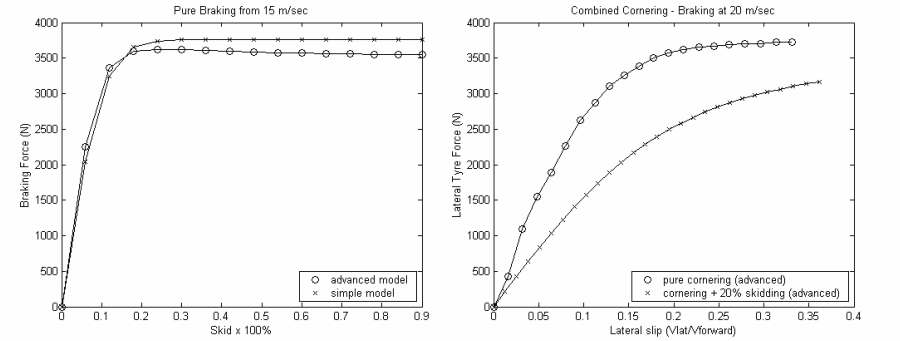

Fig. 5. Braking Force and lateral force during combined cornering - braking

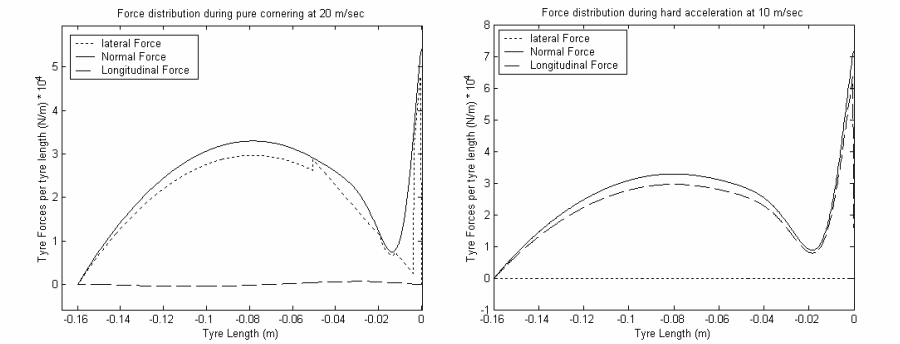

Fig. 6. Normal pressure distribution for purely cornering conditions

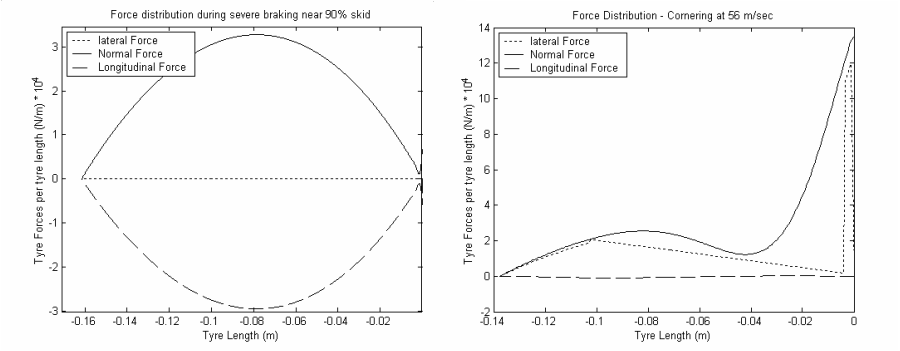

Fig. 7. Normal pressure distribution for hard acceleration and high speed cornering

Figures 6 and 7 deal with the shape of the normal pressure distribution in relation with the build up of tyre shear forces. According to the diagrams, the intensity of the impact in the beginning of the contact patch determines the shape of the Force-Slip relations. Pure cornering lies midway between traction and braking. The rolling velocity of the tyre corresponds to a forward velocity of 20 m/sec and the leading edge impact does not cause much distortion to the parabolic shape of the distribution. During hard acceleration, the increased rolling velocity causes deviations from the parabolic shape, while the opposite effect is observed during braking, when rolling velocity deteriorates. High velocity cornering, as shown in the second diagram of Figure 7, causes a higher distortion of the shape of the normal pressure distribution and this in turn effects the generation of the cornering force.

Simulation also indicates that the generation of shear forces depends largely on the initial conditions of the infinitesimal mass. Assuming a rigid tyre belt with the bristles connected to it, it is sensible to use V_{sx} and/or V_{sy} as initial velocities for the infinitesimal mass. By doing so, the mass is initially sliding and has to be decelerated by friction in order to enter the "stick" phase. This produces an area of increased friction force in the beginning of the contact patch, as shown in Figures 6 and 7.

In reality, the tyre belt deforms laterally as well as longitudinally. In case of cornering, the direction of the mass just before entering the contact patch is such that part of the circumferential velocity compensates for V_{sy}. Thus, the relative initial velocity of the mass can be less than V_{sy} and in cases of moderate cornering could even reduce to zero. Consequently, the overall friction forces decrease for the same normal pressure distribution. This finding points out a major shortcoming of brush

type models and indicates the need of their integration with a belt-carcass deformation model.

While the peak at the leading edge of the contact patch is evident in experimental results [8], it is not as intense as predicted by the current analysis. This is explained by the fact that the impact at the leading edge of the contact patch is not the only mechanism for the vertical deceleration of the mass. In fact, most of the deceleration is achieved internally, by the local deformation of the tyre belt in the neighborhood of the leading edge. Again, the need of integration of the brush model with a belt deformation model is obvious.

5 CONCLUSION

A new formulation of the generation of normal and shear tyre forces is presented. With the aid of numerical integration, a number of different operating conditions are studied and some comments are made concerning the effects of different kinds of manoeuvres - namely cornering, braking and traction - on tyre behaviour. Finally, two basic shortcomings of the brush-type models are highlighted and the effect of extremely high operating speeds is addressed.

REFERENCES

1. Pacejka H.B. and Sharp R.S.: Shear Force Development by Pneumatic Tyres in Steady-State Condition: A Review of Modelling Aspects. *Vehicle System Dynamics* 20 (1991), pp. 121-176.
2. Sakai H.: Theoretical and Experimental Studies on the Dynamic Properties of Tyres, Part 1: Review of theories of Rubber Friction. *Int. J. of Vehicle Design* 2(1) (1981), pp. 78-110.
3. Sakai H.: Theoretical and Experimental Studies on the Dynamic Properties of Tyres, Part 2: Experimental Investigation of Rubber Friction and deformation of a tyre. *Int. J. of Vehicle Design* 2(2) (1981), pp. 182-226.
4. Sakai H.: Theoretical and Experimental Studies on the Dynamic Properties of Tyres, Part 3: Calculation of the six components of force and moment of a tyre. *Int. J. of Vehicle Design* 2(3) (1981), pp. 335-372.
5. Sakai H.: Theoretical and Experimental Studies on the Dynamic Properties of Tyres, Part 4: Investigations of the influences of running conditions by calculation and experiment. *Int. J. of Vehicle Design* 3(3) (1982), pp. 333-375.
6. Bernard J.E., Segel L. and Wild R.E.: Tyre Shear Force Generation During Combined steering and Braking Maneuvers. *SAE paper 770852* (1977).
7. Sharp R.S. and El-Nashar M.A.: A Generally applicable Digital Computer Based Mathematical Model for the Generation of Shear Forces by Pneumatic Tyres. *Vehicle System Dynamics* 15 (1986), pp. 187-209.
8. Levin M.A.: Investigation of features of Tyre Rolling at Non-Small Velocities on the Basis of a Simple Tyre Model with Distributed Mass Periphery. *Vehicle System Dynamics* 23 (1994), pp. 441-466.
9. Karnopp D.: Computer Simulation of Stick-Slip Friction in Mechanical Dynamic Systems. *Transactions of the ASME – Journal of Dynamic Systems, Measurement and Control* 107, pp. 100-103.
10. Braghin F., Cheli F. and Resta F.: Friction Law Identification For Rubber Compounds on Rough Surfaces at Medium Sliding Speeds. *3rd AIMETA International Tribology conference*, Salerno, Italy, 18-20 September 2002

11. Denti Eugenio and Daniele Fanteria.: Models of Wheel Contact Dynamics: An Analytical Study on the In-Plane Transient Responses of a Brush Model. *Vehicle System Dynamics* 34 (2000), pp. 199-225.
12. Yu Zeng-Xin, Tan Hui-Feng, Du Xing-Wen and Sun-Li: A Simple Analysis Method for Contact Deformation of Rolling Tire. *Vehicle System Dynamics* 36(6) (2001), pp. 435-443.